Article citation info:
Dziubak T. Analysis of the filtration process of inlet air to an internal combustion engine in a two-stage filter. Combustion Engines. 0000;XXX(X):xx-xx. https://doi.org/10.19206/CE-207838

Tadeusz DZIUBAK

Combustion Engines
Polish Scientific Society of Combustion Engines

Analysis of the filtration process of inlet air to an internal combustion engine in a two-stage filter

ARTICLE INFO

Received: 2 June 2025
Revised: 1 July 2025
Accepted: 2 July 2025
Available online: 16 July 2025

The destructive effect of mineral dust grains (SiO_2 and Al_2O_3) on the accelerated abrasive wear of engine connections was demonstrated. It was shown that the use of two-stage (multi-cyclone-baffle) air intake filters for motor vehicle engines used in conditions of high air dustiness is necessary. The aim of the work was a theoretical and experimental analysis of the properties of paper filters operating in series behind a cyclone and without a cyclone. An original research methodology was used, which consisted of the simultaneous testing of a single cyclone and a paper filter with an appropriately selected surface area. The system tests (cyclone-paper filter) were carried out using conditions that corresponded to the actual filtration conditions in a two-stage air filter, including the filtration speed in the paper bed, the dust concentration in the air sucked into the engine, and the average cyclone inlet speed. The basic filtration characteristics of filtration efficiency, accuracy, and pressure drop of two paper filters were determined as a function of the dust mass fed to the system (cyclone-paper filter) or directly to the characteristic filter. It was found that the paper filter operating in series behind the cyclone achieves four times longer operating time, limited by a specific value of permissible resistance. In the initial (short) filtration period, lower filtration efficiency values were obtained than the required value of 99.5%. On the other hand, dust grains with a maximum size of 13.5 µm were found in the air behind the paper filter. The required filtration accuracy of the engine intake air is in the range of 2–5 µm. For this reason, the initial air filtration period is an undesirable phenomenon and may cause accelerated engine wear.

Key words: *internal combustion engine, air filter, multicyclone, paper filter, air filtration efficiency and pressure drop*

1. Introduction

The basic component of the working medium of an internal combustion engine is air taken from the atmosphere, and its quantity is proportional to the power output of the engine.

The mass of air supplied to an internal combustion engine depends on the displacement V_{ss} of its rotational speed n and the filling of the cylinder with a fresh charge, and this depends on the type of engine intake system, in which there may be a supercharging device.

For passenger car engines, the intake air flow (theoretically calculated) can be in the range of 150–400 m^3/h. Truck engines, due to their significantly larger V_{ss} displacement, achieve higher values (900-2000 m^3/h) of the intake air flow. However, the highest values of air demand (3500–6000 m^3/h) are achieved by CI engines, which are the drive unit of special vehicles, and these are tanks, armoured personnel carriers, and special units built on the chassis of these vehicles.

Various pollutants in the atmospheric air are sucked into the engine along with the intake air. The main component of engine intake air pollution is mineral dust. Its source is sandy and deserted areas and off-road areas, where trucks, special vehicles, including tracked military vehicles and work machines are used. Dust is lifted from dry ground by moving vehicles or by the wind, but after some time it falls by gravity. The concentration of dust in the air specified in the conditions of vehicle use is particularly high, often exceeding the value of 1 g/m^3 and can reach the value of 10 g/m^3.

Mineral dust has a specific chemical and granulometric origin that varies with the type of surrounding soils and location. Regardless, silicon oxide (SiO_2) and aluminum oxide (alumina), Al_2O_3 (about 10–15%), account for the largest share of dust (about 60–90%). The various oxides found in dust (Fe_2O_3, MgO, CaO, K_2O, Na_2O, SO_3) reach trace values [32]. Silicon oxide, known as silica, is a very common compound in nature. It makes up 12% of the earth's crust and is also found in minerals where it is in bound form (silicates, aluminosilicates). Then its content reaches 52% of the earth's crust. Silica is therefore a major component of sand, rocks, and soil. The most common varieties of crystalline silica in the world are quartz and cristobalite.

The chemical composition of dust depends strictly on the type and condition of the substrate (dry sandy substrate), altitude above the ground, climatic factors, as well as the type of dust fallout from fires, landfills, forests, peat bogs, and fallout from industrial dust and dust from volcanic eruptions [62].

The measure of dust content in the air is the concentration defined as the mass of dust (in grams or milligrams) contained in 1 m^3 of atmospheric air. The concentration of dust in the air is a variable quantity and depends on many factors: the type of ground (sandy, loess, grassy), vehicle movement dynamics (speed, single vehicle or convoy), the presence of other vehicles in the vicinity, weather conditions (rain, drought, wind direction), and the type of chassis (wheeled, tracked).

The dustiness of the air during vehicle operation varies with the concentration of dust in the ambient air and depends on the type of soil on the ground, vehicle movement conditions such as speed, the position of the vehicle in the convoy, and the type of running gear, as well as the type and intensity of precipitation. For this reason, the concentration of dust around a moving vehicle varies greatly.

Airborne dust concentrations can vary from 0.01 mg/m^3 in rural environments to approximately 20 g/m^3 during the movement of tracked vehicles in desert conditions on dry ground [54]. The author of [36] states that dust concentrations in the air can range from 0.001 to 10 g/m^3. According to research presented in [49], the maximum concentration of dust in the air varies widely, from 0.05 to 10 g/m^3. When vehicles are traveling on highways, the dust concentration can vary within a fairly wide range of 0.0004–0.1 g/m^3, and when a convoy of vehicles is traveling on sandy terrain, the concentration reaches 0.03–8 g/m^3 [6]. The author's research [20] shows that the dust concentration in the air measured behind a column of tracked vehicles reached a maximum value of 1.17 g/m^3. The dust concentration determined during measurements at a distance of 80 mm from the surface of the armour of a tracked vehicle used in sandy terrain at a speed of 14–18 km/h has values in the range of 2.1–3.8 g/m^3 [14]. The dust concentration increases with increasing driving speed. During the landing of a CH-53 helicopter on a landing site with sandy terrain, the dust concentration in the air at a height of about 0.5 m above the ground can reach the value of s = 3.33 g/m^3 [11]. The intake system's combustion engine intake system draws in air where the dust concentration usually does not exceed 2.5 g/m^3 [36, 49] when the vehicle travels on sandy ground.

Dust in the atmospheric air limits visibility. Dust content in the air of 0.6–0.7 g/m^3 causes a significant reduction in visibility, while if the dust content of the air exceeds 1.5 g/m^3 there is a complete lack of visibility, which is very dangerous for moving vehicles [56]. Examples of air dust concentration for various terrain conditions are shown in Fig. 1.

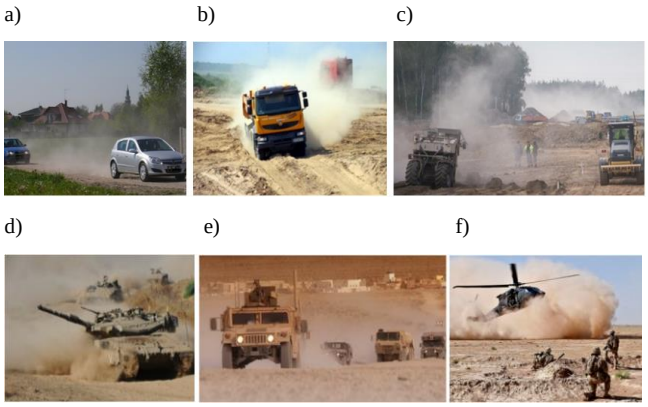

Fig. 1. Use of vehicles in high air dust levels: a) passenger cars on dirt roads, b) trucks on construction sites, c) working machines during road construction, d) tanks in desert terrain, e) military vehicles in a column in sandy terrain, f) helicopter landing in a desert [21]

The density of dust in the air depends on the type of roads and the conditions of vehicles (Fig. 2).

The highest air dust concentration (over 1,000 times higher than during vehicle traffic on city streets, highways, and paved roads) occurs during the use of tracked vehicles on dry, sandy training grounds. Dust levels are significantly higher behind a column of tracked vehicles than behind a column of wheeled vehicles, which is mainly due to the type of vehicle drive system.

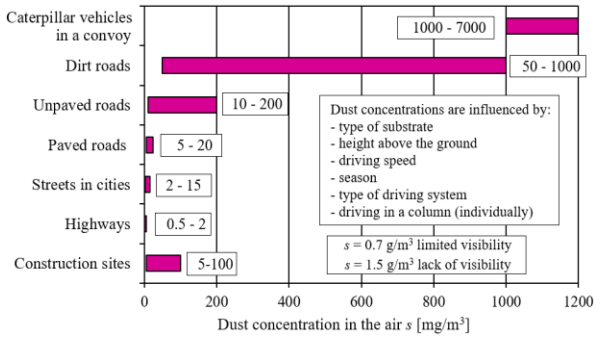

Fig. 2. Dust concentration in the air depends on the type of substrate [22]

2. The impact of dust on the wear of internal combustion engine components and its operation

The thickness of the oil film depends proportionally on the temperature of the oil and the relative velocity of the mating surfaces, and inversely proportionally on the thrust force, and therefore on the operating conditions of the engine (speed, load) and on the position of the piston between BDC and TDC and takes variable values in the range h_{min} = 0–50 μm [17]. When the piston with its rings is at the top of the cylinder (compression or work stroke) the oil film reaches its smallest values.

The high temperature of the connection elements causes a decrease in viscosity and the thickness of the oil film. In addition, the low relative speed of the piston and rings (at TDC it has the value of "0"), as well as the high load, reduce the thickness of the oil film, which leads to contact of dust grains (even those of small size) with the surfaces and their wear. This causes the highest wear of the upper part of the cylinder and the upper piston rings. Numerous literature data indicate that dust grains in the range of 1–40 μm are the main cause of excessive abrasive wear of engine parts surfaces. However, dust grains in the size range of 5–20 μm are the most dangerous for two cooperating surfaces and therefore should be removed from the intake air of engines [7, 47, 55].

The authors of [42] state that more than 30% of the pollutant mass delivered with the engine intake air stream does not participate in abrasive wear, but gets into the engine exhaust system, which causes increased emission of particulate matter (PM). On the other hand, very small dust grains can be burned at high temperatures in the cylinder. Other processes are subject to mineral dust grains, whose melting point is much lower than the temperature in the cylinder during combustion (2000–2500°C). The melting point of polymorphic varieties of SiO_2 quartz is: tridymite 1470–1710°C, and cristobalite about 1722°C. Grains of these minerals are melted and, in the form of droplets, enter the exhaust system, where they are deposited on its components. The glassy surface formed on the catalytic layer weakens the performance of the catalytic reactor [10].

Excessive wear of the P-PR-C assembly causes increased leakage in the supercharged space, which is the cause of increased blow-by of fresh charge into the crankcase during the compression stroke. This results in a drop in compression pressure and thus a drop in engine power. Leakage of the P-PR-C joint increases blow-by of exhaust gases into the crankcase, which raises the oil temperature

and increases the content of contaminants, mainly soot, accelerating oil aging [39, 64]. Excessive leakage between the P-PR-C components means a greater flux of oil above the piston, where it becomes coked up at the high temperatures found in the combustion chamber, which in turn increases particulate emissions [2, 8, 31, 41].

Dust grains contained in the air entering the engine cylinders and, in the oil, have a destructive effect on engine components, and their effects are varied and consist of (Fig. 3):

- abrasive wear of P-PR-C components
- abrasive wear of friction-operated components supplied with lubricating oil: main and connecting rod bearings (journal-bearing) of the engine crankshaft and camshaft, valve guide, camshaft cam-valve disc, pin-piston connecting rod, and valve seat
- erosive wear of the compressor and turbine
- reduction of heat exchange on the measuring element of the air flow meter by forming an insulating layer of dust and other contaminants
- reduction in the effectiveness of catalytic reactors as a result of molten dust particles settling on the catalytic surface.

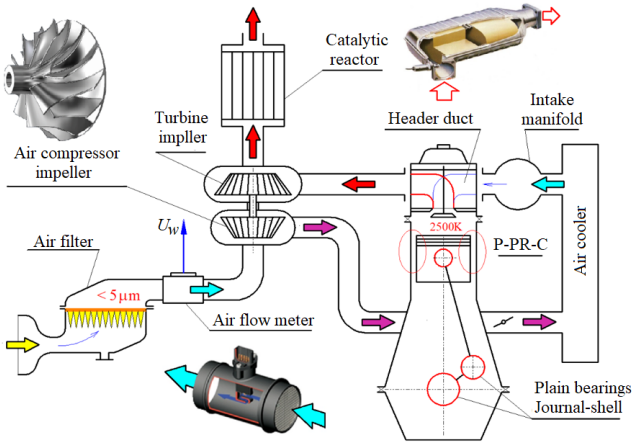

Fig. 3. Functional diagram of the intake system of a motor vehicle combustion engine and components affected by mineral dust

3. Air filtration systems in internal combustion engines

In order to ensure the required purity of the inlet air to the engine (removal of grains above the 2-5 µm range), and thus minimize excessive abrasive wear of engine components, air filters are used as part of the air supply system.

Air filters made of standard fibrous media are selective in terms of the size of the particles they retain, since not all particles are retained and collected in the filter bed with the same efficiency. For example, the authors of papers [60, 51] found a lack of penetration for particles larger than 4 µm during testing, even with new, unloaded filters.

The author of the paper [7] concludes that for all practical purposes, typical heavy-duty, high-efficiency air filters are 100% effective for particles larger than 4 to 5 µm when operating properly. These figures, combined with the information given earlier that particles smaller than 2 µm do not contribute significantly to wear of the engine's P-PR-C association, constitute the critical particle size range assumed hereafter as 2–5 µm. Particles smaller than this size range penetrate the filter but do not contribute to wear. Particles larger than the 2 to 5 µm range can be major contributors to wear, but do not penetrate high efficiency filters. The author's study of the paper [7] shows that only 14% of the particle mass according to ISO 12103-1, A1 Ultrafine Test Dust is smaller than 2 µm.

Depending on the conditions in which vehicles are used, and in particular on the value of dust concentration in the air, their engines are equipped with a single-stage (passenger cars) or two-stage (trucks and special vehicles) air filtration system. The filter element of a single-stage filter is a rectangular panel made of paper or composite materials (polyester + glass microfiber + cellulose). The pleating of the paper provides a large (about 2 m^2) filter area in a small filter body, which allows passenger cars to be used at low dust concentrations for about 30,000–50,000 km of mileage. Filter papers that are less than 1 mm thick have low dust absorption in the range (200–240 g/m^2). Therefore, they cannot be used as stand-alone air filters for a vehicle engine operating at high dust concentration in the air.

For example, the air intake of the engine of a tracked vehicle with a power of 700 kW and a displacement of V_{ss} = 38.8 dm^3, which is operated at an average speed of v = 20 km/h on sandy roads at a dust concentration of s = 1 g/m^3, sucks in about 170 kg of mineral dust with the air after 1,000 km. A passenger car engine with a much smaller displacement (V_{ss} = 1.5 dm^3) is capable of sucking in more than 0.6 kg of dust with the air if it is used over a 40,000 km mileage on paved roads, where the dust concentration in the air is only s = 5 mg/m^3.

Therefore, air-supply systems for the propulsion engines of motor vehicles, mainly military vehicles (tanks, wheeled and tracked transporters) and engineering machinery, are equipped with filters that can retain significant masses of dust from the intake air and at the same time ensuring high filtration efficiency and accuracy. These are filters with a two-stage filtration system (Fig. 4). The function of the first stage of filtration is performed by an inert filter, usually a multicyclone, although monocyclones are popularly used in truck filters. In series behind the multicyclone, forming an integral unit, is the second filtration stage for engine inlet air. This is a cylindrical filter cartridge (baffle filter) constructed of pleated paper or a component of filter materials and a surface area so selected that the velocity of flow through the bed (filtration speed) does not exceed 0.06 m/s. Constructed and operated in this way, the device primarily provides the required 99.9% efficiency and accuracy of filtration of dust grains above the range of 2–5 µm, and a slow increase in pressure drop, resulting in a long service life.

A multicyclone is a device built of individual cyclones, the internal diameters of which do not exceed D = 40 mm. The cyclones are arranged in parallel next to each other for short distances. The cyclones are arranged vertically next to each other at short distances. The cyclone's dust discharge openings are fixed to a sealed settling tank, and the purified air outlet tubes are fixed tightly to a plate that is the base of a rectangular tank, where the second-stage filter cartridge is located [23, 27, 45, 48].

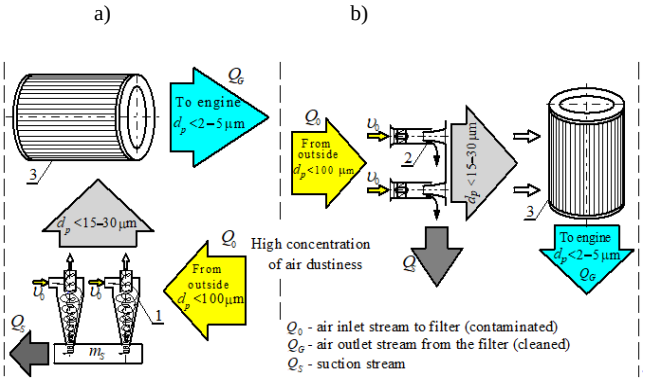

Fig. 4. Air filtration systems in a two-stage filter: a) multicyclone built of return cyclones with tangential inlet – porous baffle), b) multicyclone built of through cyclones – porous baffle

The number of cyclones in a multicyclone is from several dozen to several hundred. The multicyclone of the PT-91 tank air filter contains 108 return cyclones with a tangential inlet, and the multicyclone of the Leopard tank filter contains 288 through-flow cyclones with an axial inlet. The types of cyclones used for filtering the intake air of motor vehicle engines are shown in Fig. 5.

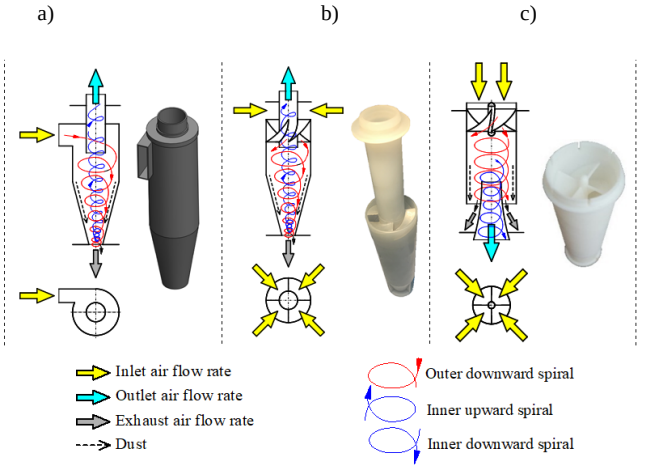

Fig. 5. Types of cyclones used for intake air filtration in motor vehicles: a) reverse cyclone with tangential inlet, b) reverse cyclone with axial inlet, c) axial flow cyclone

The second stage of filtration is a cylindrical filter cartridge made of pleated filter paper, a cheap and easy-to-process material, which is arranged in series behind the multicyclone.

The disadvantage of paper filter beds is their low initial filtration efficiency and high pressure drop, with a small mass of dust retained by the filter bed. For this reason, filter media manufacturers use composite beds made of synthetic layers and a layer of nanofibers.

A layer of nanofibers with a thickness of 1–5 μm and fibre diameters of 300–800 nm [15, 29, 33] is applied to a standard filter bed made of fibres with diameters of 10–15 μm, which improves the filtration efficiency of dust particles smaller than 5 μm in the air sucked into the engine. Examples of the design of pleated paper filter cartridges shaped into cylinders having an elliptical or circular cross-section suitable as a second filtration stage behind a multicyclone are shown in Fig. 6.

Fig. 6. Examples of designs of filter cartridges of two-stage filter

4. Air filtration process in a two-stage filter

4.1. Introduction

The essence of a two-stage filter (multicyclone-paper cartridge) is to combine the operation of two devices, where different air filtration processes take place. A multicyclone is a device that uses centrifugal force to separate solids or liquids from gas. Therefore, in a multicyclone, at a specific flow rate, only large particles (above 15–35 μm) and heavy particles will be separated from the air. Multicyclones are characterized by the ability to remove large air streams for an unlimited time without the need to handle significant amounts of dust, with an efficiency of 85–90%. As a result, only a small portion of the dust mass that was in the air sucked in from the environment flows into the filter cartridge located behind the multicyclone.

The return cyclone with tangential inlet is made of a body consisting of a cylindrical part with a diameter D and a part in the shape of an inverted cone, the smaller diameter of which is tightly connected to the dust settling chamber, where the pollutants separated in the cyclone are stored (Fig. 7). The upper part of the cylindrical body is the place of the tangentially attached inlet nozzle, which usually has a rectangular cross-section with sides “a” and “b”.

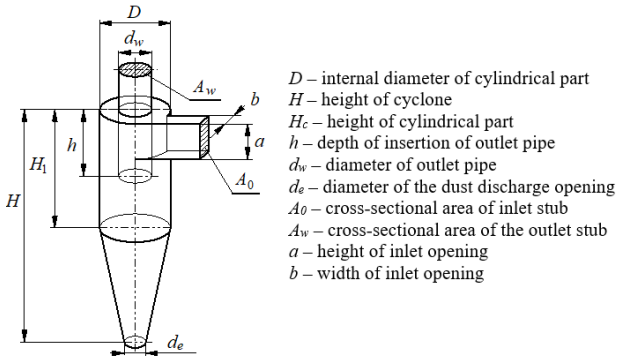

Fig. 7. Typical dimensions of a reverse cyclone with tangential inlet

The inlet pipe is positioned in relation to the cylindrical part of the cyclone so that its axis is usually perpendicular to the main axis of the cyclone, although there are cyclones with an inclined inlet pipe. The cylindrical part of the cyclone is covered tightly from the top with a circular cover, in the center of which, centrally in the vertical axis of the cyclone, is fixed tightly a cylindrical outlet tube usually with a diameter of 0.5D.

4.2. Air filtration in a multicyclone

The process of cleaning gases from solid particles carried out in a cyclone consists in introducing a stream of

contaminated gas into a rotating motion, followed by a change in the direction of the flow of the stream of contaminated air, which causes that solid particles of larger size and mass, due to their inertia, tend to follow the original direction of movement and are separated from the air, and then collect in a special settling tank, while the cleaned air together with particles of lower density or smaller size pass further. The idea of cleaning gases in a cyclone was patented by Knickerbocker Co. Jackson, USA in 1886 [61]. The design of the cyclone is very simple, but the process of aerosol filtration in the cyclone is very complicated, difficult to describe mathematically, which is mainly due to the complex vortex motion of the aerosol stream, first the screw motion of the gas (external vortex) together with the dust downwards (Fig. 8), and then the screw motion of the gas upwards (internal vortex), to the cyclone outlet [17].

Considering the movement of a dust grain in a cyclone in a plane perpendicular to the cyclone axis, it can be seen (Fig. 8) that two opposing forces act on the grain: the inertial force F_B and the aerodynamic force F_R. After several rotations, the particle meets the cyclone wall, which significantly reduces its speed. Then the particle, driven mainly by the spiral air flow, rotates along the cyclone wall and moves into the collection chamber. The effect of gravity on the particle is of little importance.

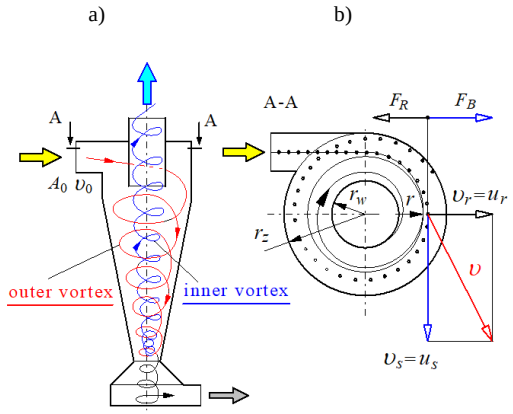

Fig. 8. Simplified model of aerosol flow in a reverse cyclone: a) vortex system, b) force system: a) vortex system, b) force system: A_0 – cross-sectional area of inlet tube, r_w – radius of outlet pipe, r_z – radius of cylindrical part, υ_0 – cyclone inlet velocity, υ_r – radial component of gas velocity in the cyclone, υ_s – tangential component of gas velocity. u_s – tangential component of grain velocity, u_r – radial component of grain velocity

The air stream is set in rotational motion in a reverse flow cyclone by feeding it tangentially into the cylindrical part of the cyclone through a special nozzle (Fig. 3a) or by flowing through stationary, obliquely positioned deflectors mounted between the inner wall of the cylindrical part and the outlet pipe (Fig. 8b). The dust separated in the cyclone is directed to the settling tank, which is tightly attached to the dust removal opening located in the lower part of the cyclone.

Excessive dust accumulation in the cyclone settling chamber is not recommended, as it may be re-sucked through the opening in the cyclone bottom. This situation may occur during vehicle shocks or sudden changes in the air flow through the cyclones, which result from rapid changes in engine speed when used on uneven terrain. Entrainment of dust from the settling chamber by the air flow rotating towards the outlet pipe results in a decrease in the cyclone filtration efficiency. To prevent this phenomenon, continuous dust removal from the settling chamber is used, using an additional air flow (Q_S suction flow), which is part of the cyclone inlet flow.

The main air stream, after being freed from dust particles of larger size and mass and flowing to the lowest zone of the cyclone, abruptly changes the direction of flow by 180 degrees, followed by a helical motion (internal vortex) flow back upward. The air stream moves upward along the cyclone's central axis and then leaves the cyclone through the outlet pipe while still performing a helical motion and lifting smaller dust particles with it. During the outflow of the air stream through the outlet tube, there are significant pressure losses, which, according to the authors of works [44, 50], reach up to 50–80% of the total pressure drop in the cyclone. Tangential inlet returns cyclones achieve a pressure drop in the range of 2–3 kPa, which is their main disadvantage. In comparison, the pressure drop of axial cyclones is much lower, reaching values of 0.5–0.7 kPa. The high pressure drop in the air supply system caused by the air filter has an adverse effect on filling the engine with fresh air, resulting in a decrease in torque and power. It can also cause excessive emissions of toxic components in the exhaust gas.

The movement of dust particles in a cyclone is usually considered only in the plane perpendicular to the cyclone axis. In this case, two forces act on the dust particle: the inertial force F_B and the aerodynamic drag force F_R (Fig. 8). Other forces also act on the dust particle in the cyclone, but their influence on the trajectory is negligible. Dust particles move along a trajectory whose shape depends on the mutual relationship between the values of F_B and F_R. In turn, the value of both forces depends on the size, shape, and material of the dust particle, as well as the type of gas flowing through the cyclone. Dust particles that have been given a spinning motion obtain the centrifugal force described by the relation:

$$F_B = \frac{m_z \cdot u_s^2}{r} \cdot \rho_g \tag{1}$$

where: m_z – mass of the dust particle, u_s – tangential component of the particle velocity approximately equal to the tangential component of the gas velocity υ_S at this point, r – distance of the dust particle from the axis of rotation.

This force causes the particle to move towards the cyclone wall at a speed u_r. This movement is counteracted by the medium resistance force F_R, determined by the relationship:

$$F_R = \lambda \cdot A_p \cdot \frac{u_r^2}{2} \cdot \rho_g \tag{2}$$

where: A_p – projection area of the grain (area of the grain projected onto a plane) in the direction of its movement, u_r – component of the radial movement of the grain, ρ_g – gas density, λ – friction coefficient depending on the shape of the grain and the Reynolds number

It is assumed that dust particles with diameters smaller than a certain dimension dpg, defined as the limiting particle diameter, for which the condition $F_B < F_R$ applies, will

enter the cyclone and be carried by the internal air vortex towards the cyclone outlet pipe. On the other hand, dust particles with diameters greater than the dpg dimension, for which $F_B > F_R$, will move along a spiral line and be directed towards the cyclone wall, and thus be separated. The balance equation of forces acting on single dust grains is expressed by the relationship [16].

$$m_p \frac{du_p}{dt} = F_R + F_B + F_G + F_M + F_C \quad (3)$$

F_M – Magnus force (created by the rotation of particles in the flow field), F_C – force created between dust particles and the inner wall of the cyclone, as well as the force generated as a result of collisions between dust particles, F_G – gravitational force.

It follows from the relationship (1) that the smaller the distance of the dust grain from the axis of rotation r (smaller diameter D of the cylindrical part of the cyclone), the greater the inertia force at the same cyclone inlet velocity υ_0 and the same dust particle mass. This results in increased efficiency and accuracy of air filtration in the cyclone. For this reason, in practice, sets of cyclones with small diameters (multicyclones) are used instead of one cyclone with a large diameter. In the air-supply systems of internal combustion engines of motor vehicles, for air pre-filtration, are used assemblies of 100–300 return or through cyclones, the internal diameter of which does not usually exceed D = 40 mm. The ends of the cyclones are mounted in common lower and upper plates, which allows for the supply of aerosol through a common pipe from the place with the lowest dust concentration. Aerosol suction by individual cyclones can also be carried out directly from the environment. Figure 9 shows a two-stage air filter for a tracked vehicle engine, where the multicyclone is constructed of return cyclones with a tangential inlet.

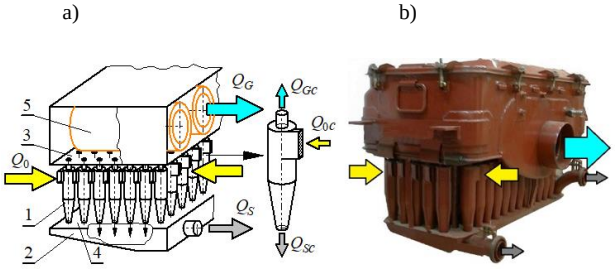

Fig. 9. Two-stage air filtration system for a tracked vehicle engine: 1 – multicyclone (return cyclones with tangential inlet), 2 – dust tank, 3, 4 – top and bottom plate fixing cyclones, 5 – paper filters of the second stage of filtration

4.3. Air filtration in a porous partition

In a porous partition, where the filter bed is made of densely packed fibres, dust particles are retained by individual fibres as a result of the simultaneous action of several filtration mechanisms: interception, inertial, diffusion, gravitational settling, and sieving [38, 70] (Fig. 10).

The interception mechanism occurs when a dust particle moving along the air stream line, flowing around the bed fibre, approaches the fibre to a distance equal to its radius and comes into physical contact with it. The inertial mechanism occurs when a heavy particle cannot adapt to sudden changes in the direction of the air stream near the fibre and, due to inertia, continues to move along its original path and then comes into contact with the fibre, where it is retained. The inertial mechanism is more effective at high particle inflow velocities [70]. The diffusion mechanism exists in laminar flow when particles do not move near the fibre along the streamline, but perform random Brownian motion, moving in directions transverse to the direction of aerosol flow, colliding with fibres and settling there. The smaller the particle size (< 0.1 μm) and their velocity, the more intensely they fall out of the stream line and the greater the likelihood of their deposition on the fibre surface.

The gravitational mechanism exists as a result of the retention of large and heavy particles with a free fall velocity. It is particularly important in vertical flow through the filter bed. The gravitational mechanism is significant for particles with a diameter greater than 1 μm flowing through the filter bed at a velocity greater than 0.05 m/s. The effect of gravity is negligible for particles smaller than 0.5 μm [5].

The total separation efficiency of the bed results from the combined effect of all filtration mechanisms. Figure 10 shows that the efficiency of the capture mechanism and the inertial mechanism increases with the size of dust grains above 0.1 μm [5]. A similar nature of the increase in filtration efficiency, but dust grains above 1 μm is presented by the sieve mechanism. In contrast, the efficiency of the diffusion mechanism has the opposite effect to the previous mechanisms. Its value decreases with increasing dust grains. For small dust grains (less than 0.1 μm), the efficiency resulting from the inertial mechanism is the highest. Therefore, the total filtration efficiency assumes a characteristic minimum in the graph (Fig. 10), from which it follows that dust particles in the range of 0.08–0.3 μm are retained by the filtration mechanisms with lower efficiency [3, 70].

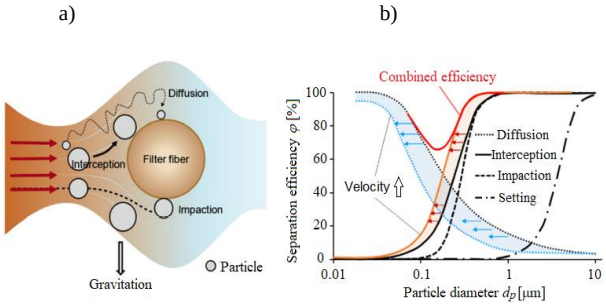

Fig. 10. Model of particle retention in a porous partition. (a) operation of filtration mechanisms on a single fibre: (b) total efficiency of filtration mechanisms [38]

The result of the filtration mechanisms in the filter bed is the retention of dust particles on the surface of the fibres of the porous structure and on previously deposited particles. This creates complex dendritic structures (agglomerates) that slowly grow and fill the free spaces between the fibres (Fig. 11). The filter cartridge made of pleated paper is characterized by high filtration efficiency (99.5–99.9%) and accuracy above 2–5 μm. The disadvantage of filter papers is their low dust absorption capacity (in the range of 220–250 g/m^2). This is due to the structure of the filter bed and its small thickness, which does not exceed g_m = 0.6–0.9 mm. The accumulation of dust on the fibres of the porous

partition causes the free spaces between the fibres to fill up (Fig. 11), which reduces the space for air flow and results in a continuous increase in pressure drop Δp_f, which, after some time, can reach significant values.

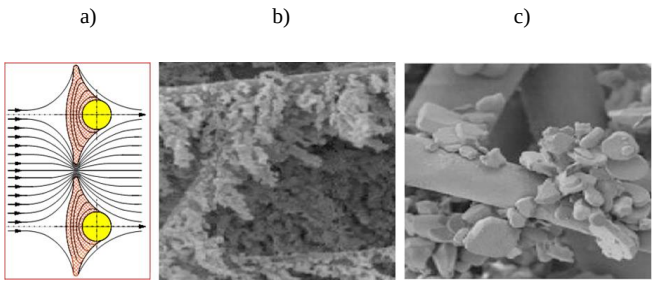

Fig. 11. View of accumulated dust particles (agglomerates) on the fibers of the filter bed: a) scheme of layer formation, b) SEM image of agglomerates formed on the fiber, c) SEM image of the bed of micron-sized aluminum oxide aerosol agglomerates [3]

This is a characteristic feature of partition filters. An increase in the pressure drop Δp_f of the filter above a specified permissible resistance value Δp_{fdop} is not recommended. This causes a decrease in the engine's fresh charge and power, and an increase in the emission of harmful exhaust components [59]. The criterion determining the permissible resistance value Δp_{fdop} of air filters is based on a 3% decrease in engine power. The experimentally determined permissible resistance values for passenger car engines are in the range of Δp_{fdop} = 2.5–4.0 kPa. For truck engines and special vehicles, these values are Δp_{fdop} = 4–7 kPa [13, 25]. In order for the filter to achieve the Δp_{fdop} value, the filter cartridge must be replaced with a new one.

Multicyclones have the fundamental advantage of being able to separate significant amounts of dust from a large air stream in a short time without affecting the pressure drop. A multicyclone does not require maintenance, and the dust collected in the sedimentation tank is systematically removed by an ejection suction system.

The combination of a multicyclone and a partition filter as a two-stage filter extends the service life of the air filtration system several times (until the value of Δp_{fdop} is reached) compared to a single-stage filter, which results in a longer vehicle mileage (Fig. 12).

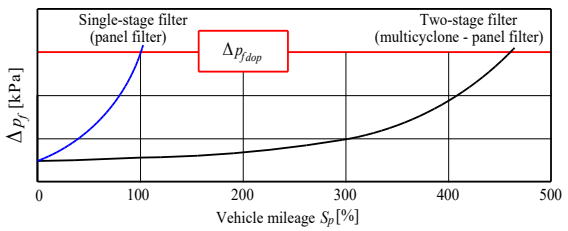

Fig. 12. Change of pressure drop of the air filter (porous membrane) and the filter with a two-stage filtration system ("multicyclone – porous membrane") as a function of vehicle mileage

In the available literature, the results of numerical and experimental studies of single return cyclones with a tangential inlet [9, 40, 66, 67] and through cyclones with an axial inlet [4, 24, 34, 69] aimed at selecting the optimal dimensions of the cyclone and its components are presented in quite large numbers. In the literature, there are, but not very many, studies of an ensemble of several or dozens of cyclones in terms of the uniformity of airflow through individual cyclones and its effect on filtration efficiency [18, 46, 68].

Computational fluid dynamics simulations coupled with experimental validation of fibre beds are being conducted to determine recommended parameter combinations for their optimal design in terms of minimizing flow resistance characteristics or increasing the filtration efficiency of filter media [28, 43]. Studies are being conducted on the effects of dust particle size distribution and filter air velocity on dust layer structure. Experimental results showed that layers containing smaller particles of equivalent mass showed increased pressure drop [65].

A considerable amount of work deals with the study of filter beds with a layer of nanofibers, which is applied to a standard filter bed (cellulose). The nanofiber layer has a thickness of 1–5 μm and fiber diameters in the range of 300–800 nm [12, 33, 57]. This improves the filtration efficiency of dust grains with a diameter of less than 5 μm in the inlet air of the engine, resulting in less wear on its components and increased durability. The results of original scale testing of internal combustion engine air filters are few [35, 42, 63], which is mainly due to the high cost of testing, as well as the availability of a test bench to produce the air flow resulting from engine operation, especially a special vehicle engine at full load.

From the above analysis, it can be seen that the performance and flow resistance characteristics of a single cyclone or cyclone unit are studied, and fibre beds are separately studied in terms of performance and flow resistance. The problem of aerosol filtration in a cyclone is quite different from that in a filter with a porous baffle, where dust accumulation causes an increase in flow resistance, which is a limitation of its further use. This problem does not exist in cyclone filters, which is a maintenance-free filter if extraction of the separated dust is used.

The combination of these two units into a single device, if a number of conditions are met, functions as a two-stage filter. However, the available literature lacks a quantitative and qualitative description of the phenomena occurring in the process of air filtration in a two-stage filter operating in a "multicyclone-baffle filter" system. The present work aims to partially fill this gap, and these are the conducted experimental studies of the two-stage air filtration system "single cyclone-paper filter". This is a novel test method, which consists of testing an assembly: a single cyclone and a paper filter set in series behind it, which has an appropriately sized filter surface to maintain the required ($\upsilon_{Fdop} \leq$ 0.06 m/s) filtration speed.

In addition, other important test conditions that characterize the actual filtration process in the original two-stage air filter were maintained. These are the filtration velocity of the original paper filter bed and the cyclone inlet velocity derived from the number of cyclones in the multicyclone and the engine inlet air flow. The test results of the paper filter bed operating directly downstream of the single cyclone can be used in the design work of two-stage filters in terms of evaluating its filtration capacity and estimating the

mileage of the vehicle limited by the achievement of acceptable pressure drop.

5. Methodology and conditions of experimental research on the "cyclone-research filter" unit

5.1. Purpose and scope of the study

Experimental tests were aimed at evaluating the properties of two filter papers covering the characteristics of filtration efficiency and accuracy, dust absorption, and pressure drop. The filter papers were pleated and then shaped into a cylindrical filter cartridge, which was placed in a housing, and the whole was named the A1 and A2 research filters (Fig. 13a).

The scope of the study was to examine the filter characteristics of the two research filters, which operated in two filtration systems (variants). The two-stage filtration system was a return cyclone and an integrally connected (arranged in series) research filter (A1 or A2). The single-stage system was a research filter without a cyclone. The filtration characteristics of the research filters (A1 and A2) were determined according to the mass of dust m_D dosed uniformly and with a specified concentration (s = 1 g/m^3) into the cyclone of the "cyclone-test filter" research unit, and in the case of single-stage operation directly into the research filter (s = 0.5 g/m^3).The other test conditions themselves were the same for both variants.

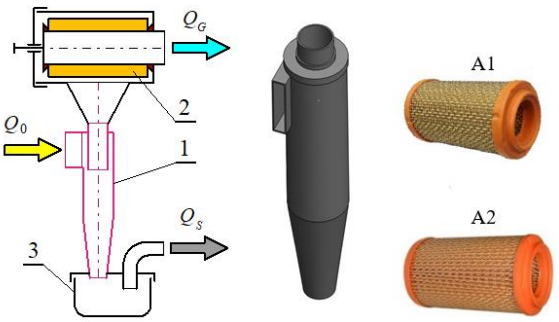

Fig. 13. Filter assembly "return cyclone - research filter": 1 – cyclone, 2 – paper filter cartridge, 3 – tank of separated dust

The reverse cyclone with a tangential inlet was the first stage of filtration in the "cyclone–test filter" filtration unit. The basic parameters of the cyclone are shown in Fig. 14a. The second stage of filtration consisted of test filters, A1 and A2, with the parameters given in Fig. 14b.

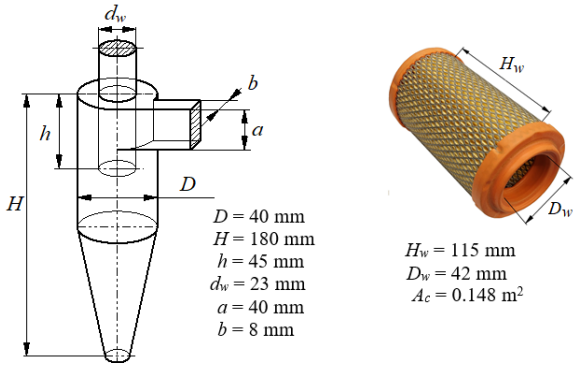

Fig. 14. Basic dimensions of a) return cyclone with tangential inlet, b) research filter

The value of the air flow rate Q_G flowing through a single cyclone was determined as the quotient of the air flow rate Q_{Silmax} flowing into the engine for speed n_N and the number of return cyclones with tangential inlet in the multicyclone for which the baffle filter is selected. In the case of the cyclone under study, this value is Q_G = 34 m^3/h. The Ac surface area of the filter paper of the test filter was selected from the condition of the permissible (maximum) filtration velocity, which for filter papers used for the second stage of filtration should not exceed the value $\upsilon_{Fdop} \leq 0.06$ m/s. A cylindrical test filter was made from the calculated A_c surface of the paper (Fig. 14b). Two test filters were made, each from a different filter paper (made by J.C. BINZER), which were named A1 and A2, respectively. The parameters of the cartridges are given in Fig. 14. The papers differed in the values of the structure parameters (Table 1). The A1 filter paper has six times higher pressure drop than the A2 paper, due to its higher grammage (204 g/m^2) and smaller (42 μm) diameter. Filters made in this way were the subject of research in the "reverse cyclone-filter research" team.

Table 1. Basic parameters of filter paper manufactured by J.C. BINZER Papierfabrik, used to make filter cartridges for testing

Parameters	Units	Paper identification	
		A1	A2
Grammage	g/m^2	204	108
Thickness - load 2 N/cm^2	mm	0.9	0.67
Pressure drop at 400 cm^3/s, A = 10 cm^2	mbar	6.7	1.04
Tearing strength	kPa	385	212
Resin content	%	18.8	17
Maximum value of pore diameter	μm	51	89
Average value of pore diameter	μm	42	76

Experimental tests were performed on the characteristics of A1 and A2 test filters operating as a second stage of filtration in a "cyclone-test filter" unit and without a cyclone. The tests were carried out using PTC-D test dust while maintaining a constant flux value of Q_G = 34 m^3/h, which corresponds to the actual filtration velocity $\upsilon_F \leq$ 0.0638 m/s. The following characteristics were studied:

– filtration efficiency $\varphi_w = f(m_D)$
– pressure drop $\Delta p_w = f(m_D)$

where: m_D – dust mass dosed uniformly to the "cyclone-test filter" unit or directly to the test filter.

– filtration accuracy $d_{pmax} = f(m_D)$.

Since dust grains are retained in the filter bed selectively in terms of particle size, in the air downstream of the filter, their size also varies from d_{pmin} to d_{pmax}, with dust grains of the smallest size being the largest. Therefore, in this study, the criterion for filtration accuracy is the dust grain with the largest size found in the air behind the filter and is designated d_{pmax}. The number of dust grains in the air behind the filter under study and their sizes, including the size of the dust grain d_{pmax}, were determined in each measurement cycle using a particle counter.

5.2. Experimental research methodology

The tests were carried out on a test stand (Fig. 15), the main components of which are a return cyclone with

a tangential inlet and a test filter (A1 or A2) located behind it in series.

The suction fan forces the air stream Q_G flowing in the "cyclone-test filter" unit. To measure the Q_G flow rate, and mass flow meter with a measuring range of 10–150 m^3/h and an accuracy of 1.2% was used. A dust extraction system pipe is connected to the dust settling tank, together with a safety filter and a rotameter, which is used to measure the Q_S extraction flux. A rotameter with a measuring range of 1–7 m^3/h and an accuracy of 0.01 m^3/h was used. To determine the pressure drop Δp_w of the test filter, a water pressure gauge U-tube connected after the test filter at a distance of $6d_w$ (d_w – filter outlet diameter), where the values of pressure drop Δh_m after the filter were recorded. To protect the flow meter sensor from dust, there is an absolute filter in the measuring line, which is also a filter for measuring the mass of dust passed through the filter.

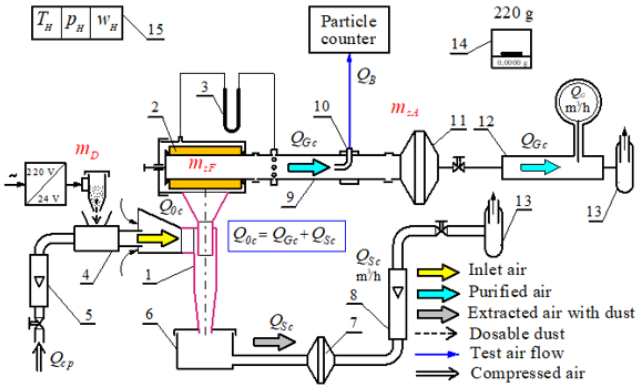

1 – cyclone, 2 – measuring filter, 3 – U-tube manometer, 4 – dust dispenser, 5 – compressed air rotameter, 6 – dust settling tank, 7 – absolute filter, 8 – suction flow rotameter, 9 – measuring tube, 10 – dust measuring probe, 11 – measuring (safety) filter, 12 – air mass flow meter, 13 – suction fans, 14 – analytical balance, 15 – device for measuring air humidity, temperature and ambient pressure

Fig. 15. Diagram of the test stand for the "cyclone-filter test" assembly

The experimental tests were performed using polydisperse PTC-D test dust, which is suitable in Poland for testing air filters in motor vehicle engines as a substitute for AC fine test dust. The chemical and granulometric composition of PTC-D dust is consistent with AC fine dust in terms of particle sizes below 80 µm. The mass content of particles smaller than 10 µm in the total dust mass is over 50%. These are particles that are very difficult to retain by filtration systems. The chemical and fractional composition of PTC-D dust is given in Table 2 and Table 3.

Table 2. Chemical composition of PTC-D dust

Dust component	SiO_2	Al_2O_3	Fe_2O_3	Na_2O	K_2O	CaO	MgO	moisture
Mass content in dust [%]	67.15	15.25	4.9	4.5	4.5	2.35	1.15	3

Table 3. fractional composition of PTC-D dust

Dust grain size d_p [µm]	0÷5	5÷10	10÷20	20÷40	40÷80
Mass share of dust fraction U_m [%]	38.55	15.97	16.48	19.46	9.54

Of note is the high (more than 50%) content in the dust of grains below 10 µm and the fact that more than 67% of the dust by weight is SiO_2, which is a mineral of high hardness.

During the testing of the characteristics of filters A1 and A2 operating in a single-stage and two-stage filtration system, the following conditions were applied:

– outlet air flow from the test filter Q_G = 34 m^3/h
– suction flow Q_S is defined as 10% of the outlet air flow from the Q_G filter
– dust concentration for the inlet stream to the cyclone s = 1 g/m^3
– dust concentration for the inlet stream (single-stage filtration) to the test filter s = 0.5 g/m^3
– mass filtration efficiency of the cyclone used for testing φ_c = 92%.

Filtration characteristics: efficiency $\varphi_w = f(m_D)$ and filtration accuracy $d_{pmax} = f(m_D)$ as well as pressure drop $\Delta p_f = f(m_D)$ were determined for a constant air flow rate Q_G. The same measurement cycles j of a fixed duration were performed sequentially, during which dust was evenly dosed into the test system. The measurement duration was set to τ_p = 120 s in the initial period. During the main operating period of the filters, the duration was extended to τ_p = 240–480 s. The number and size of dust particles in the air behind the filter were recorded by a particle counter.

After each test cycle, j, measurements were made of the quantities that were necessary to determine the characteristics: efficiency and filtration accuracy, pressure drop, and actual dust concentration in the inlet air stream.

The filtration efficiency of the test filters was determined by the gravimetric method as the quotient of the mass of dust m_{zFj} retained by the filter and the mass of dust m_{DFj} dosed uniformly over a specified time to the test unit (measurement cycle j) using the relation:

$$\varphi_j = \frac{m_{zFj}}{m_{DFj}} = \frac{m_{zFj}}{m_{zFj}+m_{zAj}} 100\% \quad (4)$$

where: m_{zAj} – mass of dust retained on the absolute filter during the next "j" measurement cycle.

The mass of dust retained on the test filter cartridge during the next "j" measurement cycle was determined from the relation:

$$m_{zFj} = m''_{zFj} - m'_{zFj}, \quad (5)$$

where: m''_{zFj}, m'_{zFj} – the mass of the test filter after (before) the measurement.

The mass of dust retained on the absolute filter during the next "j" measurement cycle was determined from the relation:

$$m_{zFj} = m''_{zAj} - m'_{zAj}, \quad (6)$$

where: m''_{zAj}, m'_{zAj} – the mass of the absolute filter, after the measurement and before the measurement, respectively.

The dust mass retained on the research filter m_{zFj} and the absolute filter m_{zAj} and the mass dosed to the m_D unit were determined using an analytical balance with a measuring range of 220 g and an accuracy of 0.0001 g.

2. Filtration accuracy was determined as the largest dust grain size $d_{pj} = d_{pmax}$ in the air stream behind the filter.

3. The pressure drops Δp_{fj} of the research filter was determined as the static pressure drop before and after the filter based on the measured height Δh_{mj} on a U-tube water manometer according to the relationship:

$$\Delta p_{wj} = \frac{\Delta h_{mj}}{1000} \cdot (\rho_m - \rho_H) \cdot g \text{ [Pa]} \quad (7)$$

where: Δh_{mj} – height measured on a U-tube water manometer after the end of dust dosing, ρ_m – density of the manometric liquid [kg/m^3], ρ_H – air density [kg/m^3], g – gravity [m/s^2].
4. The amount of N_{zi} dust particles in the purified air downstream of the filter was measured within established size ranges (d_{pimin}-d_{pimax}).
5. For a given test cycle, the percentage fraction (d_{pimin} – d_{pimax}) of dust grains in the air stream was calculated from the following relationship:

$$U_{zi} = \frac{N_{zi}}{N_z} = \frac{N_{zi}}{\sum_{i=1}^{32} N_{zi}} 100\%, \quad (8)$$

where: $N_z = \sum_{i=1}^{32} N_{zi}$ – total amount of dust particles in the air cleaned after the filter during one measurement cycle
6. The actual dust concentration in the cyclone inlet air was determined after the test using the quantities measured during the test and applying the relation:

$$s = \frac{3600 \cdot m_D}{(Q_G + Q_S) \cdot \tau_p} \text{ [g/m}^3\text{]} \quad (9)$$

According to the above methodology, the filtration characteristics were determined: efficiency $\varphi_w = f(m_D)$ and filtration accuracy $d_{pmax} = f(m_D)$ and pressure drop $\Delta p_w = f(m_D)$ of the A1, A2 research filters operating in a single- and two-stage system. The criterion for completing the tests was that the test filter (A1, A2) achieved the established set value of acceptable resistance Δp_{fdop}.

6. Results of experimental studies and their analysis

The results of the filtration efficiency $\varphi_w = f(m_D)$, filtration accuracy $d_{pmax} = f(m_D)$, and pressure drop $\Delta p_w = f(m_D)$ tests of test filters A1 and A2, which operated as a single-stage filter (without a cyclone) and as a second stage of filtration (after a reverse cyclone), are presented in Fig. 16–18. The filtration characteristics were determined as a function of the dust mass m_D supplied to the "cyclone-test filter" test unit or directly to the test filter. The filtration efficiency characteristics $\varphi_w = f(m_D)$ and pressure drop characteristics $\Delta p_w = f(m_D)$ of test filters A1 and A2, which were the second stage of filtration after the reverse cyclone, are shown in Figure 16. Despite the same test conditions, the characteristics of both tested filters differ across the entire range in terms of values and performance, which is mainly due to the different parameters of the filter paper structure (Table 1) used to make the test filters.

The main difference in the course of the characteristics can be seen in the first (initial) period of filtration, which is designated conventionally (F_{A1}, F_{A2}). This period is called the transient filtration period in the literature. Its characteristic feature is small values of filtration efficiency. Filters A1 and A2 achieve an initial filtration efficiency of φ_{wA1} = 71.1% and φ_{wA2} = 50.6%, respectively. However, with the amount of dust mass retained by the filter paper, the filtration efficiency increases steadily, with the intensity of the increase for the two filters studied being different.

It was assumed for the purposes of this study that the criterion for the end of the initial filtration period (the transient filtration period) is that the paper achieves a filtration efficiency of φ_w = 99.5%. Within the framework of this study, it was assumed that the criterion for the end of the initial (interim) filtration period is that the paper reaches the filtration efficiency φ_w = 99.5%. The above conventional value was adopted based on the work of [7, 30, 36, 54], where the presented test results indicate that an increase in filtration efficiency above the range φ_w = 99.5–99.9% clearly reduces engine wear. Figure 16 shows the dependence of the filtration efficiency of a typical air filter over its full-service life fed with AC fine dust and the resulting engine wear in the form of a normalized wear index. As the filter's operating time increases, the efficiency increases, resulting in a decrease in the abrasive wear of the engine and thus an increase in its service life. From the course of both curves, it can be seen that reaching a filtration efficiency of φ_w = 99.9%, the intensity of engine wear decreases significantly. If the filter is serviced at 100% of its design life, engine wear is minimized (the normalized wear rate is 1.0), and the filtration efficiency reaches the design level of ~99.97% (Fig. 16). The graph indicates the increasing rate of engine wear resulting from servicing the air filter more often than necessary.

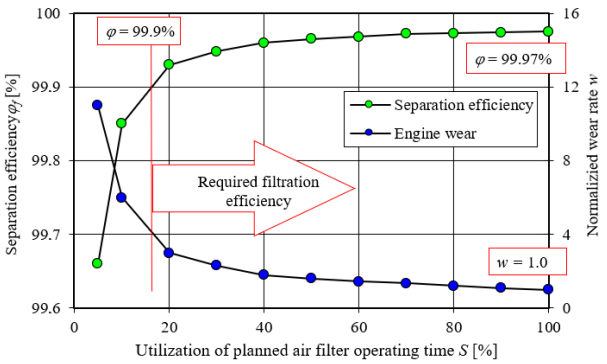

Fig. 16. Filtration efficiency and relative value of engine wear as a function of air filter operating time [7, 30]

Figure 17 shows the rate of abrasive wear of the cylinder liner and piston ring when three air filters with different filtration efficiency are used compared to when no air filter is installed in the engine.

Any air filter with higher efficiency reduces the wear of both engine components dramatically, with the wear rate of the piston ring being several times higher than that of the cylinder liner. Taking the abrasive wear of both the cylinder liner and piston ring without an air filter as 100% (Fig. 17), using an air filter with 97.8% efficiency reduces the wear of both components to 1.89%. After using an air filter with a higher efficiency of 99.45% and 99.42%, the wear of the cylinder liner and piston ring is only 0.41% and 0.43%, respectively, compared to the wear when there was no air filter in the engine. Hence, the reasonableness of taking the

filtration efficiency of 99.5% as the required minimum value for the cleanliness of the engine's inlet air.

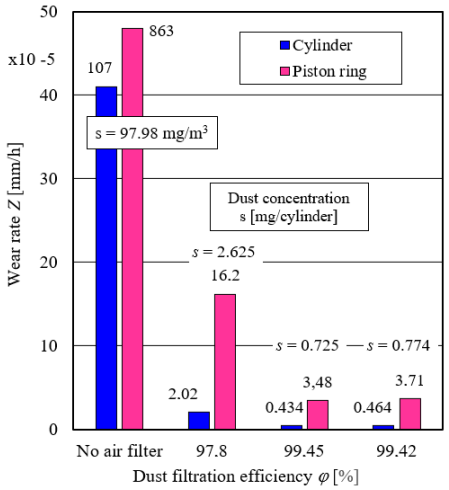

Fig. 17. Effect of air filter efficiency on the wear rate of cylinder liner and piston rings compared to no air filter [1]

The test results shown in Fig. 18 prove that the initial filtration period for the A1 filter is much shorter than that of the A2 filter. This is due to the different values of the parameters of the filter paper structure and the filtration process that takes place in it. The paper of the A1 filter has twice the grammage, which is due to the greater packing of the fibers, and thus the pore diameters obtain smaller values. For this reason, the A1 filter's conventional filtration efficiency (φ_w = 99.5%) is achieved after retaining m_{DA1} = 16.82 g of dust, while the mass of dust retained by the A2 filter until it achieves (φ_w = 99.5%) has a value of m_{DA2} = 35.78 g, twice as much.

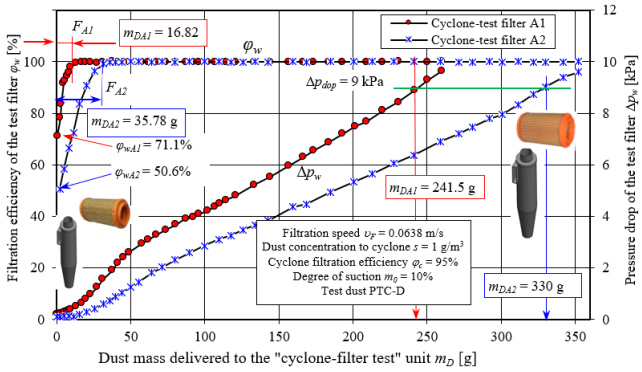

Fig. 18. Characteristics $\varphi_w = f(m_D)$, $d_{pmax} = f(m_D)$ and $\Delta p_w = f(m_D)$ of test filters A1 and A2 depending on the mass of dust mD delivered to the "return cyclone-test filter A1 (A2)" unit

The operation of the filtration mechanisms in A1 paper is more efficient. Dust particles retained by the direct hooking and inertial mechanism more intensively form tree-like dendritic clusters on the fibers, which fill the free spaces (pores) between the fibers. The consequence of this phenomenon is the impeded aerosol flow between fibers, an increase in flow velocity, and an increase in pressure drop, which is a function of velocity to the second power. The inherent phenomenon of dust mass retention by the filter bed is an increase in pressure drop. On the other hand, the dendrites growing on the fibers reduce the distance between adjacent fibers, resulting in the retention of smaller and smaller dust grains. This phenomenon should be explained by the continuous increase in filtration efficiency and accuracy. In the initial period of filtration, dust grains with a maximum size of d_{pmax} = 13.3 µm were recorded in the air behind the A1 filter, after which the size of these grains decreases and for a dust mass of m_{DA1} = 16.82 g has a value of only d_{pmax} = 2.3 µm (Fig. 19). On the other hand, for the A2 filter, the maximum size of dust grains in the purified air has a value of d_{pmax} = 13.5 µm, but dust grains with a size of d_{pmax} = 2.7 µm were recorded only after m_{DA2} = 64.17 g of dust was delivered to the system.

Dust filtration phenomena occurring in the filter bed cause changes in filtration efficiency and accuracy and are closely related to changes in pressure drop. Therefore, the pressure drop of filter A1 increases more intensively than that of filter A2. The different intensity of the increase in pressure drop causes the A1 filter to achieve a pressure drop value of Δp_w = 9 kPa, when a mass of dust (m_{DA1} = 241.5 g) is delivered to the test assembly. Filter A2, due to a less intense increase in pressure drop, the value of Δp_w = 9 kPa was obtained much later than filter A1, which is related to the dust mass m_{DA2} = 330 g delivered to the "cyclone-filter test" assembly.

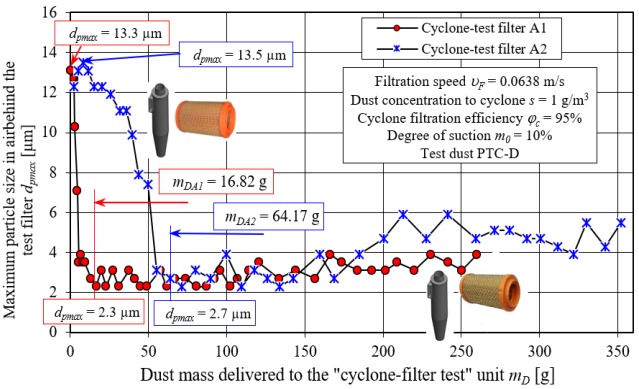

Fig. 19. Characteristics $d_{pmax} = f(m_D)$ of test filters A1 and A2 depending on the mass of dust m_D delivered to the "return cyclone-test filter A1 (A2)" unit

For this reason, in the air stream flowing out of the test filter, the number of N_{zp} dust grains was recorded during each measurement, starting with measurement No. 1, in a dozen fixed same measurement channels, which were limited by fixed $d_{pmin} - d_{pmax}$ grain sizes (Fig. 20) ranging from 0.7 µm to 80 µm. It was found that for a given measurement, the number of dust grains in the air behind the filter with increasingly larger diameters decreased until they were completely absent (Figure 20). The dust grain located in the last dimension channel has the largest size $d_p = d_{pmax}$ and is an indication of filtration accuracy.

During the tests, it was assumed that the air filtration accuracy is determined in each measurement cycle and is expressed by the diameter of the largest dust grain d_{pmax} found in the stream of cleaned air leaving the filter.

Figure 20 shows the change in the number of dust grains depending on their size, d_{pmax}, for subsequent test cycles distinguished by the dust mass m_D retained on the filter during the preliminary (unsteady) filtration period of the A1 test filter. Measurement cycle No. 1 showed that the air behind the A1 test filter contained dust grains with a maximum size d_{pmax} = 13.3 µm.

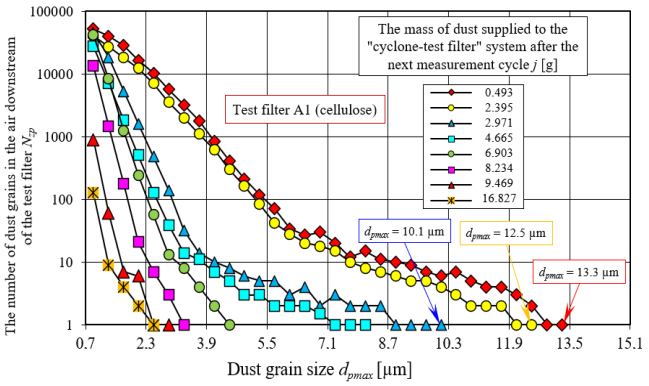

Fig. 20. Number of dust grains Nzp in the air behind the A1 filter insert depending on their size for subsequent test cycles (dust mass m_D) during unsteady filtration

Each subsequent measurement cycle showed that the total number of dust grains N_{zp} decreases, and the diameters of dust grains with a maximum size d_{pmax} are smaller and smaller. This phenomenon should be explained by the formation of dendrites on the fibres, which reduces the space for free flow and causes the retention of dust grains of smaller and smaller sizes. In the second test cycle, this is a grain size d_{pmax} = 12.3 µm, and after the third d_{pmax} = 10.1 µm (Fig. 20).

The diameter d_{pmax} = 2.3 µm, which is the smallest value of the dust grain behind the filter, was found after 16.82 g of dust was supplied to the system together with the air. This is also the moment when the filter achieved a filtration efficiency of 99.9%, which is the condition for ending the initial filtration period for the A1 filter.

The main filtration period following the initial filtration period is characterized by stabilization of filtration efficiency at the level of 99.95–99.99% and stabilization of maximum diameter sizes in the range of d_{pmax} = 2.3–3.9 µm for both filters (Fig. 20). In the final stage of the A2 filter operation, dust grains of increasingly larger sizes appear in the exhaust air but not exceeding 5.9 µm.

The above phenomenon is due to the fact that the deposit of dust grains on the fibers causes the growth of dendrites, which reduces the free flow of air and results in an increase in flow velocity. Exposed and susceptible to greater flow, the tops of the dendrites are destroyed, and detached dust grains, and sometimes significant parts of dust agglomerates, move deeper and deeper in the filter bed with the direction of air flow until they completely leave the bed. Signs of such a phenomenon were recorded during the study.

The resistance to flow of the tested research filters (A1, A2) increases all the time, which is due to the accumulation of dust and the filling of the free spaces between the fibres, resulting in a smaller airflow space, and thus a higher speed. Larger values of pressure drop Δp_w and higher intensity of growth were obtained for A1 paper. This should be explained by smaller (42 µm) pore diameters than in A2 paper (76 µm), which is associated with lower dust absorption and much lower paper permeability.

The filtration characteristics that were experimentally determined for the A1 test filter, which was the second filtration stage in the "cyclone-test filter" unit, and the characteristics of the A1 filter without a cyclone (single-stage filtration) are shown in Fig. 21.

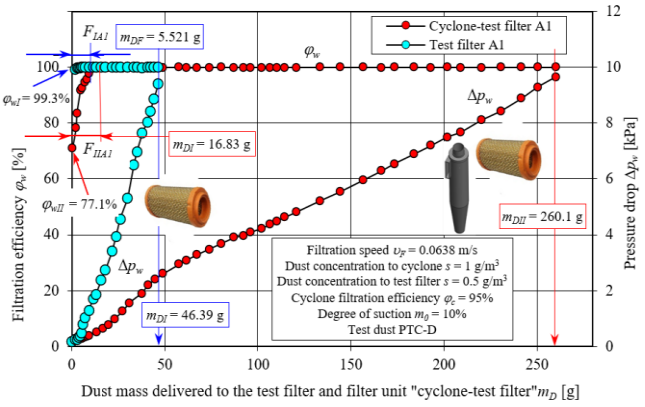

Fig. 21. Characteristics of filtration efficiency $\varphi_w = f(m_D)$ and pressure drop $\Delta p_w = f(m_D)$ of the research filter A1 as a function of the dust mass m_D supplied to the "reverse cyclone-research filter A1" assembly and to the research filter A1 without a cyclone

Significant differences can be observed as to the value and course of the characteristics $\varphi_w = f(m_D)$ and $\Delta p_w = f(m_D)$ of the A1 filter tested in different configurations.

If the test filter is operated individually (without a cyclone) it achieves high (φ_{wI} = 99.3%) initial filtration efficiency. This is due to the fact that dust grains of large size, in this case less than 80 µm, flow onto the bed. Large grains are retained mainly by the inertia mechanism and direct hooking more quickly forms dendrites on the fibres, which restrict the flow between the fibres.

The above phenomenon simultaneously increases the filtration efficiency of the tested filter, resulting in a shorter initial filtration period. Achieving an efficiency of φ_w = 99.5% ends when dust with a mass of m_{DF} = 5.521 g is delivered to Filter A1. In contrast, when Filter A1 operated as a second stage of filtration, the initial efficiency was much lower at φ_{wII} = 71.1%, and during the initial period, m_{DII} = 16.83 g of dust was delivered to the filter.

Regardless of whether the A1 filter operates without a cyclone or in a "cyclone-paper filter" unit, the pressure drop increases steadily with the amount of dust mass delivered with the air. However, the intensity of the increase in both cases is different, and therefore, the A1 filter operating without a cyclone achieves a pressure drop of Δp_{wI} = 9.6 kPa after delivering m_{DF} = 46.39 g of dust. The same value of pressure drop is obtained by filter A1 operating in a "cyclone-test filter" unit after delivering m_{DF} = 260.1 g of dust to its filter bed. This value is five times higher than that of the A2 filter. The results presented and the phenomenon described (Fig. 19) clearly explain the idea of air filtration in a two-stage filter (multicyclone-paper filter). This

makes the mileage of the vehicle until the execution of obtaining an acceptable value of pressure drop and the associated servicing of the air filter (replacement of the filter element) significantly increased.

In the case of single-stage filtration (filter operation without a cyclone), dust flows directly from the environment along with the air onto the filter bed.

When testing the characteristics of a test filter operating without a cyclone (single-stage filtration), test dust is dosed directly onto the filter bed, which corresponds to drawing air with dust directly from the environment. The inlet air contained dust grains with maximum sizes not exceeding d_{pmax} = 80 μm. On the other hand, in a two-stage filter (multi-cyclone-paper filter), the air with dust from the environment first reaches the cyclone, where the separation of dust grains of higher density and size takes place as a result of turbulence, as a result of which the dust at the outlet of the cyclone has a completely different granulometric composition than at the inlet to the cyclone (Fig. 22).

Depending on the filtration conditions, dust grains with sizes above d_p = 15–35 μm are retained in cyclones. The largest share of U_p = 16.2% in the total number of grains in the inlet air stream Q_0 to the cyclone was for dust grains with a size of 4 μm (Fig. 22). The filtration of the air in the cyclone resulted in the largest share of U_p = 36.1% in the cyclone exhaust air for dust grains with a size of 0.7 μm. As the size of the dust grains increases, their shares decrease sharply, and the share of d_p = 4 μm grains was reduced to 7% (Fig. 22).

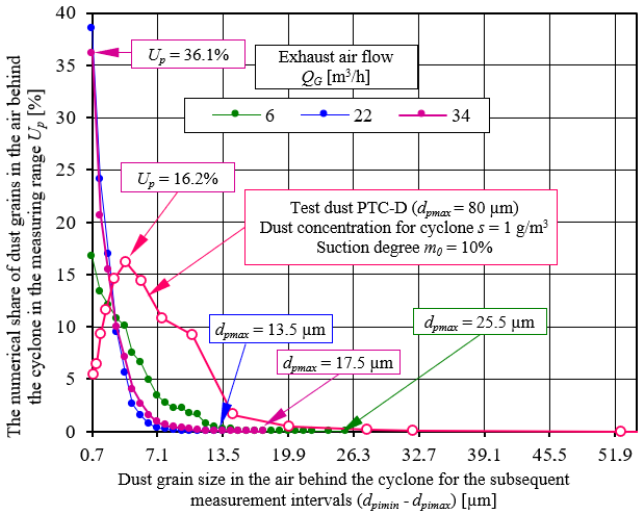

Fig. 22. Fractional composition of dust $U_{pi} = f(d_p)$ in the inlet air stream Q_0 and outlet air stream Q_0 of a reverse cyclone with a tangential inlet

This causes dust grains of smaller size and mass to be directed to the second filtration stage (paper filter), which are slower to form dendrites on the fibres and fill the space between the fibres [19, 26, 37, 52, 53, 58].

Measurements were made once, which is due to the specifics of the air filter testing methodology, so calculation of standard deviations and related standard uncertainties determined by the type A method is impossible. As for the standard uncertainties determined by the B-type method, they were due to the accuracy of the dust mass measurement assumed on the basis of the technical documentation of the balance as 0.0001 g.

Comparing the ranges of permissible variability of the obtained values of the weighted mass (±0.0001 g) with the values of the mass assumed for determining the value of filtration efficiency, it was found that the resulting uncertainties of the obtained results are at least several orders of magnitude smaller than these results (for relative uncertainties at the level of 0.012–0.021%). In view of the above, it can be concluded that the uncertainty values are small enough not to affect the obtained results.

7. Conclusions

The aim of the work was a theoretical and experimental analysis of the air filtration process in a two-stage filter, which was performed using an original research methodology consisting in testing a single cyclone and a research filter placed in series behind it, with an appropriately selected filter paper surface. The filtration characteristics were tested as a function of the dust mass fed to the system (cyclone-paper filter) or directly to the research filter. Two filters, A1 and A2, differing in paper structure, were used. During the tests, the same filtration conditions were maintained, including filtration speed, dust concentration, and cyclone inlet speed, as during filtration in a real two-stage air filter. The tests of the "single cyclone-barrier filter" assembly showed that the use of an inertial filter (multicyclone) as the first stage of filtration is beneficial due to the removal of a significant mass (85–95%) of dust from the engine intake air.

Studies of the “single cyclone-baffle filter” assembly have shown that the use of an inertia filter (multi-cyclone) as the first stage of filtration is advantageous, due to the fact that the removal of a significant mass (85-95%) of dust from the engine's inlet air extends the time of efficient operation of the two-stage filter several times.

The analysis and experimental research carried out led to the following conclusions:

1. Filter materials operating in the "cyclone-research filter" system are characterized by a less intensive increase in pressure drop and reach the permissible pressure drop 2–4 times slower than the same materials operating in a single-stage filtration system, despite the same mass m_D supplied to the system.
2. The first (initial) stage of operation of the tested filters has low (φ_w = 50–70%) filtration efficiency and low filtration accuracy, as evidenced by large (d_{pmax} = 13.5 μm) dust grains in the cleaned air. This phenomenon occurs regardless of whether the filter operates in a two-stage system (after the cyclone) or a single-stage system.
3. Lower filtration efficiency values during the initial filtration period and lower intensity of its growth occur for the filter operating in a two-stage system. Therefore, the operating time of this filter until the efficiency value (φ_w = 99.5%) is reached, which was established as the end of the initial period, lasts much longer. This is due to the fact that dust of smaller size is directed from the cyclone to the partition filter operating in the two-stage system. Dust of such granulation is difficult to retain by filtration mechanisms.

4. The initial period phenomenon is characteristic of each partition filter that starts working with dust. Such a period occurs after replacing the filter element with a new one. During this time, the air exhausted from the filter (air intake to the engine) contains dust grains whose sizes are significantly above the required filtration accuracy d_{pmax} = 2–5 μm. For this reason, this phenomenon is particularly dangerous, as it can cause accelerated wear of the piston-cylinder ring (P-PR-C) connection elements and other friction pairs lubricated with oil, which reduces the durability of the engine. It is advisable to replace the engine intake air filter element with a low frequency.
5. The developed research methodology allows for the experimental determination of basic characteristics of filter materials intended for the second stage of air filtration with any structural parameters and in a wide range of changes in filtration conditions corresponding to the operation of the air filter in conditions of high dust concentration in the air.
6. The originality of the research methodology lies in the fact that the filter material constituting the second stage of filtration is contaminated with dust whose chemical and granulometric composition has been changed and shaped as a result of the actual air filtration process in the cyclone.

Acknowledgements

This work was financed/co-financed by Military University of Technology under research project UGBWIM_22012025_15.

Nomenclature

BDC	bottom dead center
d_{pmax}	filtration accuracy
F_B	centrifugal force
F_R	air resistance force
P-PR-C	piston-piston ring-cylinder
TDC	top dead center
φ_w	filtration efficiency
Δp_f	pressure drop
Q_G	extraction flow
Q_S	exhaust air stream

Bibliography

[1] Alfadhli A, Alazemi A, Khorshid, E. Numerical minimisation of abrasive-dust wear in internal combustion engines. Int J Surf Sci Eng. 2020;14;68-88. https://doi.org/10.1504/IJSURFSE.2020.10027562

[2] Andrych-Zalewska M, Chłopek Z, Merkisz J, Pielecha J. Determination of characteristics of pollutant emission from a vehicle engine under traffic conditions in the engine. Combustion Engines. 2022;191(4):58-65. https://doi.org/10.19206/CE-147327

[3] Ardkapan SR, Johnson MS, Yazdi S, Afshari A, Bergsøe NC. Filtration efficiency of an electrostatic fibrous filter: studying filtration dependency on ultrafine particle exposure and composition. J Aerosol Sci. 2014;72;14-20. https://doi.org/10.1016/j.jaerosci.2014.02.002

[4] Babaoğlu NU, Hosseini SH, Ahmadi G, Elsayed K. The effect of axial cyclone inlet velocity and geometrical dimensions on the flow pattern, performance, and acoustic noise. Powder Technol. 2022;407:117692. https://doi.org/10.1016/j.powtec.2022.117692

[5] Bai H, Qian X, Fan J, Shi Y, Duo Y, Guo C et al. Theoretical model of single fiber efficiency and the effect of microstructure on fibrous filtration performance: a review. Ind Eng Chem Res. 2021;60(1):3-36. https://doi.org/10.1021/acs.iecr.0c04400

[6] Barbolini M, Di Pauli F, Traina M. Simulation der Luftfiltration zur Auslegung von Filterelementen. MTZ – Motortechnische Zeitschrift. 2014;5(11):52-57. https://doi.org/10.1007/s35146-014-0556-5

[7] Barris MA. Total Filtration™. The influence of filter selection on engine wear. Emissions and performance. SAE Technical Paper 952557. 1995. https://doi.org/10.4271/952557

[8] Bastuck T, Böhnke F, Hoppe S, Mittler R. Systemische Kolbenringauslegung zur Reduzierung von Partikelrohemissionen. MTZ – Motortechnische Zeitschrift. 2020;81(10): 50-55. https://doi.org/10.1007/s35146-020-0283-z

[9] Bayareh M. A review of the experimental analysis of gas–solid cyclone separators. ChemBioEng Rev. 2024;11(6). https://doi.org/10.1002/cben.202400036

[10] Bojdo N, Filippone A. a simple model to assess the role of dust composition and size on deposition in rotorcraft engines. Aerospace. 2019;6(4),44:1-26. https://doi.org/10.3390/aerospace6040044

[11] Bojdo N. Rotorcraft engine air particle separation. A thesis submitted to the for the degree of Doctor of Philosophy. Faculty of Engineering and Physical Sciences, University of Manchester. 2012. https://pure.manchester.ac.uk/ws/portalfiles/portal/38538381/FULL_TEXT.pdf (accessed 01 June 2025).

[12] Borojeni IA, Gajewski G, Riahi RA. Application of electrospun nonwoven fibers in air filters. Fibers. 2022;10:15. https://doi.org/10.3390/fib10020015

[13] Bugli NJ, Green GS. Performance and benefits of zero maintenance air induction systems. SAE Trans. 2005;114: 1015-1028. https://doi.org/10.4271/2005-01-1139

[14] Burda S, Chodnikiewicz Z. Konstrukcja i badania pyłowe filtrów powietrza silnika czołgowego(in Polish). Biuletyn WAT. 1962;3(115):12-34.

[15] Cai RR, Li SZ, Zhang LZ, Lei Y. Fabrication and performance of a stable micro/nano composite electret filter for effective PM2.5 capture. Sci Total Environ. 2020;7225: 138297. https://doi.org/10.1016/j.scitotenv.2020.138297

[16] Chen X, Yu J, Zhang Y. The use of axial cyclone separator in the separation of wax from natural gas: a theoretical approach. Energy Rep. 2021;7:2615-2624. https://doi.org/10.1016/j.egyr.2021.05.006

[17] Dehdarinejad E, Bayareh M. An overview of numerical simulations on gas-solid cyclone separators with tangential inlet. ChemBioEng Rev. 2021;8(4):1118. https://doi.org/10.1002/cben.202000034

[18] Dziubak T. Experimental studies of dust suction irregularity from multi-cyclone dust collector of two-stage air filter. Energies. 2021;14:3577. https://doi.org/10.3390/en14123577

[19] Dziubak T. Experimental dust absorption study in automotive engine inlet air filter materials. Materials. 2024;17: 3249. https://doi.org/10.3390/ma17133249
[20] Dziubak T. Zapylenie powietrza wokół pojazdu terenowego (in Polish). Wojskowy Przegląd Techniczny. 1990;3(257): 154-157.
[21] Dziubak T, Ślęzak M. Characteristics of pollutants emitted by motor vehicles and their impact on the environment and engine operation. Combustion Engines. 2025;200(1):37-55. https://doi.org/10.19206/CE-194628
[22] Dziubak T. Analysis of the influence of air pollution in the intake air of the combustion engine on the wear of its components and operation. Motor Transport. 2024;70(2):3-21. https://doi.org/10.5604/01.3001.0054.8182
[23] Dziubak T. Theoretical and experimental studies of uneven dust suction from a multi-cyclone settling tank in a two-stage air filter. Energies. 2021;14:8396. https://doi.org/10.3390/en14248396. 13.12.2021
[24] Dziubak S, Małachowski J, Dziubak T, Tomaszewski M. Numerical studies of an axial flow cyclone with ongoing removal of separated dust by suction from the settling tank. Chem Eng Res Des. 2024;208:29-51. https://doi.org/10.1016/j.cherd.2024.05.044
[25] Dziubak T, Boruta G. Experimental and theoretical research on pressure drop changes in a two-stage air filter used in tracked vehicle engine. Separations. 2021;8(71). https://doi.org/10.3390/separations8060071
[26] Fotovati S, Tafreshi HV, Pourdeyhimi B. A macroscale model for simulating pressure drop and collection efficiency of pleated filters over time. Sep Purif Technol. 2012;98:344-355. https://doi.org/10.1016/j.seppur.2012.07.009
[27] Fushimi C, Yato K, Sakai M, Kawano T, Kita T. Recent progress in efficient gas–solid cyclone separators with a high solids loading for large-scale fluidized beds. KONA Powder Part J. 2021;38;94-109. https://doi.org/10.14356/kona.2021001
[28] Gao J, Wang W, Cao Ch, Huang L, Hou Y, Xu Y et al. The relationship between the resistance characteristics and structural parameters of the elongated filter cartridge in the dust collector. Energy and Built Environment. 2024 https://doi.org/10.1016/j.enbenv.2024.03.008
[29] Grafe T, Gogins M, Barris M, Schaefer J, Canepa R. Nanofibers in filtration applications in transportation. Filtration 2001 International Conference and Exposition, Chicago. December 3-5, 2001.
[30] Graham K, Ouyang M, Raether T, Grafe T, Mc Donald B, Knauf P. Polymeric nanofibers in air filtration applications. Proceedings of the 5th Annual Technical Conference & Expo of the American Filtration & Separations Society, Galveston, 9–12 April 2002.
[31] Gunkel M, Frensch M, Robota A, Gelhausen R. Innermotorische Emissionsreduzierung Zusammenhang zwischen Partikelemissionen und Ölverbrauch. MTZ – Motortechnische Zeitschrift. 2018;79(7-8):46-51. https://doi.org/10.1007/s35146-018-0044-4
[32] Haig CW, Hursthouse A, Mc Ilwaina S, Sykes D. The effect of particle agglomeration and attrition on the separation efficiency of a Stairmand cyclone. Powder Technol. 2014;258; 110-124. https://doi.org/10.1016/j.powtec.2014.03.008
[33] Heikkilä P, Sipilä A, Peltola M, Harlin A. Electrospun PA-66 coating on textile surfaces. Text Res J. 2007;77(11):864-870. https://doi.org/10.1177/0040517507078241
[34] Huang L, Deng S, Chen Z, Guan J, Chen M. Numerical analysis of a novel gas-liquid pre-separation cyclone. Sep Purif Technol. 2018;194:470-479. https://doi.org/10.1016/j.seppur.2017.11.066
[35] Jaroszczyk T, Fallon SL, Dorgan JE, Moy JJ, Sonsalla TP, Henke B. Development of high dust capacity multi-media engine air filters. Fluid/Particle Separation Journal. 2003; 15(2):57-65.
[36] Jaroszczyk T, Pardue BA, Heckel SP, Kallsen KJ. Engine air cleaner filtration performance – theoretical and experimental background of testing. AFS Fourteenth Annual Technical Conference and Exposition, May 1, 2001, Tampa, Florida.
[37] Jeon W, Lee BH, Yun H, Kim J, Kang S, Seo Y. Characterization of pressure drop through two-stage particulate air filters. Sci Technol Built Environ. 2020;26:835-843. https://doi.org/10.1080/23744731.2020.1738870
[38] Jung S, Kim J. Advanced design of fiber-based particulate filters: materials, morphology, and construction of fibrous assembly. Polymers. 2020;12(8):1714. https://doi.org/10.3390/polym12081714
[39] Koszałka G, Suchecki A. Changes in blow-by and compression pressure of a diesel engine during a bench durability test. Combustion Engines. 2013;154(3):34-39. https://doi.org/10.19206/CE-116983
[40] Kumar M, Prakasa O, Brar LS. Analyzing the impact of inclined single and multi-inlet configurations on the turbulent flow field in cyclone separators using large-eddy simulation. Sep Purif Technol. 2025;376:134111. https://doi.org/10.1016/j.seppur.2025.134111
[41] Lensch-Franzen Ch, Gohl M, Scholl P, Paoloni F. Einfluss der Flüchtigkeit von Schmierölen auf die Öl- und Partikelemissionen. MTZ – Motortechnische Zeitschrift. 2019;80(9):46-55. https://doi.org/10.1007/s35146-019-0090-6
[42] Long J, Tang M, Sun Z, Liang Y, Hu J. Dust loading performance of a novel submicro-fiber composite filter medium for engine. Materials. 2018;11(10):2038. https://doi.org/10.3390/ma11102038
[43] Mercier Ch, Kirsch R, Antonyuk S. Analytical model for the initial efficiency of compressed nonwoven electret media for air filtration. Chem Eng Res Des. 2025l;216:549-563. https://doi.org/10.1016/j.cherd.2025.01.032
[44] Misiulia D, Elsayed K, Andersson AG. Geometry optimization of a deswirler for cyclone separator in terms of pressure drop using CFD and artificial neural network. Sep Purif Technol. 2017;185:10-23. https://doi.org/10.1016/j.seppur.2017.05.025
[45] Muschelknautz U. Comparing efficiency per volume of uniflow cyclones and standard cyclones. Chemie Ingenieur Technik. 2020;93(1-2):91-107. https://doi.org/10.1002/cite.202000149
[46] Muschelknautz U. Design criteria for multicyclones in a limited space. Powder Technol. 2019;357: https://doi.org/10.1016/j.powtec.2019.08.057
[47] Nagy J. Filtrowanie a żywotność silnika. Silniki Spalinowe 1973;3:43-47 (in Polish).
[48] Nejad JVN, Kheradmand S. The effect of arrangement in multi-cyclone filters on performance and the uniformity of fluid and particle flow distribution. Powder Technol. 2022; 399:117191. https://doi.org/10.1016/j.powtec.2022.117191
[49] Pinnick RG, Fernandez G, Hinds BD, Bruce CW, Schaefer KW, Pendelton JD. Dust generated by vehicular traffic on unpaved roadways: sizes and infrared extinction characteristics. Aerosol Sci Technol. 1985;4:99-121. https://doi.org/10.1080/02786828508959042
[50] Raoufi A, Shams M, Farzaneh M, Ebrahimi R. Numerical simulation and optimization of fluid flow in cyclone vortex finder. Chem Eng Process Process Intensif. 2008;47:128-137. https://doi.org/10.1016/j.cep.2007.08.004

[51] Reinhart C, Weisert L, Measurement of engine air cleaner efficiency using airborne particle size analysis. SAE Technical Paper 831262, 1983. https://doi.org/10.4271/831262
[52] Saleh AM, Tafreshi HV. Semi-numerical model for predicting the service life of pleated filters. Sep Purif Technol. 2014;137:94-108. https://doi.org/10.1016/j.seppur.2014.09.029
[53] Saleh AM, Fotovati S, Tafreshi HV, Pourdeyhimi B. Modeling service life of pleated filters exposed to poly-dispersed aerosols. Powder Technol. 2014;266:79-89. https://doi.org/10.1016/j.powtec.2014.06.011
[54] Schaeffer JW, Olson LM. Air filtration media for transportation applications. Filtr Separat. 1998;35(2):124-129. https://doi.org/10.1016/S0015-1882(97)80292-3
[55] Smialek JL, Archer FA, Garlick RG. Turbine airfoil degradation in the Persian Gulf War. The Journal of The Minerals Metals & Materials Society (TMS). 1994;46(12):39-41. https://doi.org/10.1007/BF03222663
[56] Szczepankowski A, Szymczak J, Przysowa R. The effect of a dusty environment upon performance and operating parameters of aircraft gas turbine engines. Conference: Specialists' Meeting – Impact of Volcanic Ash Clouds on Military Operations NATO AVT-272-RSM-047 Vilnius. May 2017. https://doi.org/10.14339/STO-MP-AVT-272-06-PDF
[57] Tian X, Ou Q, Liu J, Liang Y, Pui DY. Particle loading characteristics of a two-stage filtration system. Sep Purif Technol. 2019;215,351-359. https://doi.org/10.1016/j.seppur.2019.01.033
[58] Thomas D, Penicot P, Contal P, Leclerc D, Vendel J. Clogging of fibrous filters by solid aerosol particles Experimental and modelling study. Chem Eng Sci. 2001;56:3549-3561. https://doi.org/10.1016/S0009-2509(01)00041-0
[59] Trautmann P, Durst M, Pelz A, Moser N. High performance nanofibre coated filter media for engine intake air filtration. Proceedings of the AFS 2005 Conference and Expo, Rosemont. 10–13 April 2005.
[60] Treuhaft M, The use of radioactive tracer technology to measure engine ring wear in response to dust ingestion. SAE Technical Paper 930019, 1993. https://doi.org/10.4271/930019
[61] van Benthum R. Investigation towards the efficiency of a multi-cyclone dust separator in biomass combustion. Eindhoven, August 2007. Available online: https://www.scribd.com/document/537185062/8394 (accessed on 01 June 2025).
[62] Vogel A, Durant AJ, Cassiani M, Clarkson RJ, Slaby M, Diplas S et al. Simulation of volcanic ash ingestion into a large aero engine: particle–fan interactions. ASME J Turbomach. 2019;141(1):011010. https://doi.org/10.1115/1.4041464
[63] Wang Q, Lin X, Chen DR. Effect of dust loading rate on the loading characteristics of high efficiency filter media. Powder Technol. 2016;287:20-28. https://doi.org/10.1016/j.powtec.2015.09.032
[64] Wróblewski P. Technology for obtaining asymmetries of stereometric shapes of the sealing rings sliding surfaces for selected anti-wear coatings. SAE Technical Paper 2020-01-2229, 2020. https://doi.org/10.4271/2020-01-2229
[65] Yu W, Chen F, Li M, Cao H, Wu X, Ji Z. Experimental study on dynamic evolution characteristics of dust layer structure based on curing method. Ind Eng Chem Res. 2025; 64:4568-4580. https://doi.org/10.1021/acs.iecr.4c04727
[66] Zhang Y, Li K, Zhang K, Zhu G, Sun Z, Shi J. Research on the flow field characteristics of the industrial elliptical cyclone separator. Separations. 2025;12(50): https://doi.org/10.3390/separations12020050
[67] Zhang W, Zhang L, Yang J, Hao X, Guan G, Gao Z. An experimental modeling of cyclone separator efficiency with PCA-PSO-SVR algorithm. Powder Technol. 2019;347:114-124. https://doi.org/10.1016/j.powtec.2019.01.070
[68] Zhou X, Cheng L, Wang Q, Luo Z, Cen K. Non-uniform distribution of gas–solid flow through six parallel cyclones in a CFB system: an experimental study. Particuology. 2012; 10:170-175. https://doi.org/10.1016/j.partic.2011.10.006
[69] Zhu DZ, Han D, He WF, Chen JJ, Ji YY, Peng T et al. Optimization and assessment of the comprehensive performance of an axial separator by response surface methodology. J Appl Fluid Mech. 2023;16(1):61-73. https://doi.org/10.47176/jafm.16.01.1367
[70] Zhu M, Han J, Wang F, Shao W, Xiong R, Zhang Q et al. Electrospun nanofibers membranes for effective air filtration. Macromol Mater Eng. 2017;302:1600353. https://doi.org/10.1002/mame.201600353

Prof. Tadeusz Dziubak, DSc., DEng. – Faculty of Mechanical Engineering, Military University of Technology, Warsaw, Poland.
e-mail: *tadeusz.dziubak@wat.edu.pl*